

Molecular dynamics simulations of the ribosome - role of ArfB in ribosome rescue

Akanksha Yadav

Lab Rotation - II Report

Supervisor: Prof. Helmut Grubmüller
Co-Supervisor: Lars Bock

March 03, 2020 - April 30, 2020

Summary

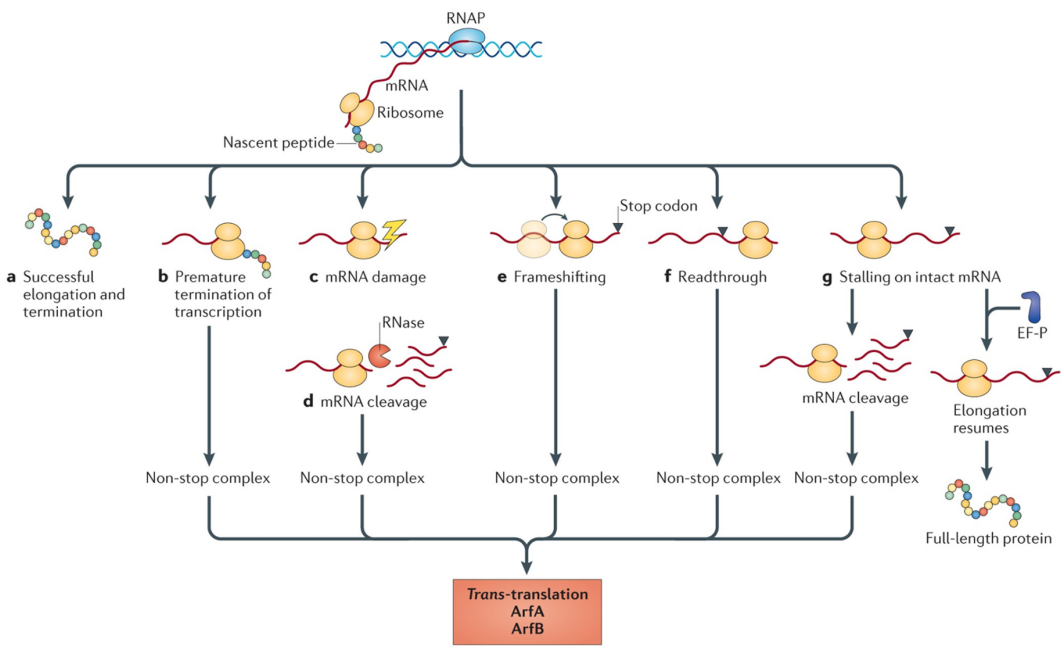
Bacteria expend a huge part of their energy and resources on efficient protein synthesis via the translation cycle. But occasionally, stalling of the ribosome on the mRNA occurs, and hence rescue systems are found across most bacterial species for recycling stalled ribosome complexes, hence ensuring cell viability [1]. Ribosomes stalled at 3' end of the mRNA with an empty A site, form non-stop complexes and are unable to elongate or terminate due to lack of codon. Three ribosome rescue systems have been identified to resolve this issue, namely (i) trans-translation mediated by transfer-messenger RNA (tmRNA) and small protein B (SmpB), (ii) rescue via alternative ribosome-rescue factors ArfA (along with peptide chain release factor, RF2) and (iii) ArfB. Since these rescue systems are specific to bacteria, small molecules that can inhibit recycling of non-stop ribosome complexes may have putative antibacterial activity.

Based on structural studies of these rescue factors (SmpB, ArfA, ArfB) and release factors (RF1, RF2, RF3) in complex with the ribosome, there is some insight into possible interactions that lead to binding and eventual peptidyl-tRNA hydrolysis (PTH) at the peptidyltransferase center (PTC) of the large ribosomal subunit. Although understanding of the entire mechanism involving the dynamics of the subunits and initial binding events that would lead to change in conformation and accommodation of these factors in the A site is still lacking.

Time-resolved cryo-EM is enabling one to visualise transient intermediates in complex processes. Our collaborators used this method to obtain a structure of ArfB bound to 70S ribosome with a tRNA carrying a dipeptide in the P site and a short mRNA. We used all-atom molecular dynamics simulations of the complex as well as of free ArfB in explicit solvent to gain further insight into the molecular mechanism of its PTH activity. We were able to observe the dynamic nature of the C-terminal tail of ArfB which explains why it is unresolved in the solution structure of YaeJ (old *E. coli* name) [pdb 2JY9]. We also saw that the GGQ loop that folds into an α -helical structure in the ribosome complex and is crucial for PTH, opens up in solution in the absence of the ribosome. With regard to ArfB in the ribosome complex, we think the role of the flexible linker joining the N-terminal globular domain and the C-terminal tail is important in the positioning of NTD for successful catalysis, but the mechanism of action is more complex than a pulling force exerted by the CTD.

1 Introduction

Bacterial growth is limited by its capacity to synthesize proteins and hence bacteria have evolved an efficient translation cycle. Occurrence of non-stop ribosome complexes, in which the ribosome stalls at the 3' end of the mRNA is a frequent event in bacteria [2]. This is a result of the fact that an empty A site cannot be elongated or terminated. It could arise due to various reasons as summarized in Fig. 1, such as premature termination of transcription, mRNA damage due to RNase activity, non-programmed frame-shifting or read-through of the stop codon. Accumulation of ribosomes into non-stop complexes would naturally compromise the translation efficiency and cell viability [1]. Hence, one or the other ribosome rescue systems that resolve non-stop complexes are present in almost all bacterial species.



Nature Reviews | Microbiology

Figure 1: Schematic of possible triggers (b-g) to formation of non-stop complexes in bacterial cells, adopted from [3]

1.1 Bacterial ribosome rescue systems

There are three rescue systems in bacteria that have been identified. One of the most ubiquitous and well-characterized rescue system is termed as trans-translation mediated by tmRNA and SmpB. The tmRNA serves as a canonical alanyl-tRNA via its tRNA-like domain (TLD) and re-initiates translation. Its messenger-like domain (MLD) encodes a short peptide with a stop codon that is added to the elongating nascent polypeptide chain during trans-translation [4]. Release of the ribosome occurs via canonical termination by RF1 or RF2. A protein-based pathway that operates as a backup rescue system for trans-translation is brought about by ArfA and RF2. RF2 is recruited by ArfA to hydrolyse peptidyl-tRNA on non-stop complexes after its initial recognition and binding

near the mRNA channel of a non-stop complex [5]. Another alternative rescue mechanism is brought about by ArfB by itself, owing to its GGQ domain that shows peptidyl-tRNA hydrolase activity similar to RFs [6].

1.2 ArfB

ArfA and ArfB were identified as products of the genes *yhdL* and *yaeJ*, respectively in *E. coli* that functioned independently of the tmRNA system. ArfB, when overexpressed, competes with tmRNA to rescue non-stop complexes and also suppresses synthetic lethality in cells with dysfunctional tmRNA and ArfA rescue systems [6],[7]. ArfB is classified as a putative release factor because of sequence similarity with domain III of class 1 release factors RF 1 and 2. The conserved GGQ motif catalyzes the hydrolysis of the aminoacyl ester bond in the peptidyl-tRNA, although it lacks any residue that interacts with stop codon and hence is much shorter in length (140 amino acids). ArfB homologs are identified in many gram-negative bacteria as well as in eukaryotes [6]. The human homolog found in the mitochondria is the immature colon carcinoma transcript-1 (ICT1)[8]. One available solution structure of ArfB [pdb 2JY9] indicates an unstructured C-terminal tail with positively-charged residues which is of particular interest because of its possible interaction with the mRNA entry channel upon binding.

1.3 Structural and functional aspects of ArfB in a non-stop ribosome complex

A recent study [9] indicates the precise molecular mechanism of the peptidyl-tRNA hydrolysis reaction catalyzed by RF 1 and 2 via interactions with the GGQ motif using quantum mechanical calculations. Structures of reaction intermediates were derived using density functional theory methods and hence the exact distances between participating atoms can now be well-defined with respect to PTH activity catalyzed via GGQ motif, as indicated in Fig. 2(i). As this GGQ motif is also conserved in ArfB, it is most likely to follow the same reaction mechanism, and hence we extrapolate the results from the above study into our analyses.

Two key studies establish most of our knowledge about interactions of ArfB with the ribosome complex [10] and about specific residues that are important for PTH activity and hence its ability to rescue stalled non-stop ribosome complexes [11]. The co-crystal structure of ArfB bound to *T. thermophilus* ribosome as discussed in [10], highlights the importance of the C-terminal tail that forms an α helix in the mRNA entry channel, but was previously seen as disordered in the solution structure [pdb 2JY9]. G530 in the 16S rRNA was observed to switch from syn to anti conformation by stacking upon Arg118 in the tail, similar to standard decoding and termination in the decoding center. Other interactions mentioned include stacking of Pro110 with A1493 and interaction of a hook-like structure in the C-terminus (residues 129-133) with 16S rRNA central pseudoknot. It was also observed that the GGQ loop becomes ordered upon binding and adopts an α -helical structure. Following the observations, they propose a model in which the C-terminus acts as a sensor for non-stop complexes based on the occupancy of the mRNA

channel. Upon binding the tail would serve as an anchor, connected via a flexible linker, while the GGQ domain samples conformations that support catalysis of PTH. Biochemical data [6],[7] also support the fact as binding of the tail is essential for peptide release.

The extensive biochemical study [6],[7],[11] indicated key residues required for *in vitro* PTH activity by performing mutational analyses. The GGQ motif is absolutely required for PTH activity. Other important GGQ domain residues are the same as in RFs based on homology. ArfB specific residues identified as important were Arg118, Leu119, Lys122, Lys129 in the C-terminal extension, Arg132 in the C-terminal tail, and Arg105 (and Thr108 to a lesser extent) in the linker region. The length of linker region is also critical as shown in Fig 2.(ii)A. Mutation in Pro110 on the other hand has a minor effect.

Hence, both these studies throw light into the importance of the C-terminal tail but further studies are required to elucidate the molecular mechanism by which ArfB or its C-terminal tail first enters the A-site of stalled ribosomes. The aim of the following study is to understand the behaviour of the domains of ArfB in solution as opposed to in the complex and also to examine physical mechanisms by which the C-terminal tail of ArfB helps in positioning the N-terminal domain for performing PTH.

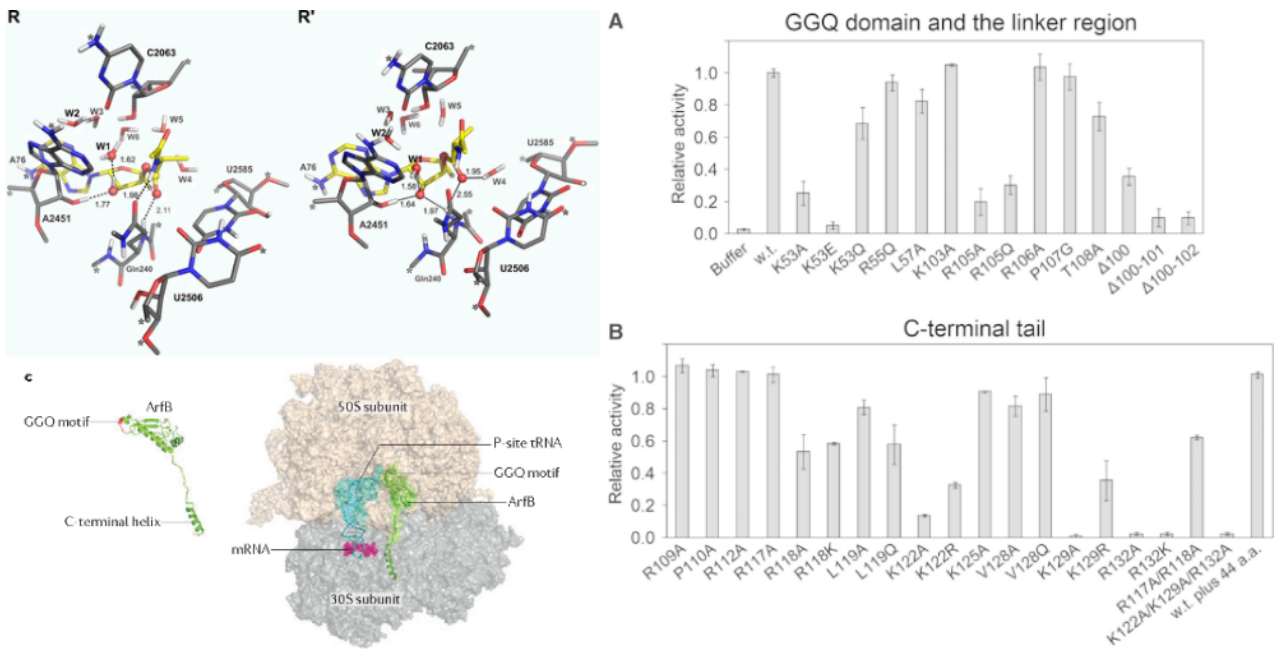


Figure 2: (i) Obtained from [9] illustrating a computational model of the PTH reaction, showing optimized reactant state R (ii) Mutants analyses as summarised in [11] with respect to PTH activity of ArfB in non-stop ribosome complex *in vitro* (iii) Cartoon representation of the crystal structure solved by [3] depicting structural aspects of ArfB in a non-stop complex. Figures adapted from [9],[11],[3] respectively

2 Methods

2.1 Ribosome complex MD simulations

We obtained a cryo-EM structure of *E. coli* 70S ribosome in complex with ArfB, a short (7nt) mRNA and a tRNA in the P-site from our collaborators, Niels Fischer and Holger Stark, before and after the peptidyl-tRNA hydrolysis step. We used the structure post-hydrolysis, which had ArfB positioned in the A site due to addition of an antibiotic, to perform an all-atom molecular dynamics simulation of the complex in order to gain insight into finer motions within domains that are important with respect to PTH activity. To test the previously reported mechanism about the plausible role of the C-terminus of ArfB in acting as an anchor to help position the N-terminal GGQ domain [10] in the PTC, we built another system from the above complex. To test whether a physical force/pull was being exerted by the C-terminus of ArfB, we introduced a 'cut' in the linker joining the globular domain with the C-terminal tail. Thus we built two starting structures for the simulations namely, "rib_arfb_full" and "rib_arfb_cut" from the initial cryo-EM structure.

The post-hydrolysis complex is the closest state to the hydrolysis reaction intermediate that was obtained but it lacks the dipeptide that is lost immediately during the reaction. To model the reaction intermediate including the intact dipeptide right before the reaction, we used the pre-hydrolysis complex structure for extracting the dipeptide structure. Hence modifications were done to the post-hydrolysis cryo-EM structure mentioned above prior to preparing the systems. This includes removal of peptide antibiotic, rigid body fitting of the acceptor stem (residues 1-7 and 66-72) of the tRNA (chain w) from the structure of ribosome without ArfB prior to hydrolysis to the cryo-EM structure (post-hydrolysis) and re-adding the dipeptide to the tRNA in our model. Further fitting of the methionine in the N-terminus of dipeptide was done using a structure of *E.coli* ribosome [pdb: 5AFI][12] to add the N-formyl group (FME). The "rib_arfb_cut" system differed from the above system in residues 101 and 102 of ArfB (chain y). Glu101 and Lys102 were replaced by uncharged common termini NH₂ and ACE respectively.

All the molecular dynamics simulations were performed using the GROMACS software version 2018 [13] using amber99sb force field and SPC/E water model as established previously in the lab. [14] Parameters for ions were also obtained as in the previous study. The systems were prepared by placing the complexes in a dodecahedron box with a 1.5 nm spare boundary and adding water molecules. Mg²⁺ and Cl⁻ ions were added using GENION from the GROMACS package to resemble a concentration of 7mM followed by K⁺ and Cl⁻ ions with a concentration of 150 mM to neutralize the system.

We ran five independent simulations each for the two systems here on using the same protocol as followed in [14]. This involved initial equilibration in 4 steps before the final production run - (i) Steepest descent energy minimization to resolve atomic clashes (ii) 0-50ns: Positional restraint on all atoms from the structure (force constant $k = 1000 \text{ kJ/mol/nm}^2$) to equilibrate solvent and ions (iii) 50-70ns: Linear release of position restraint to finally perform free production run (iii) 70-670ns: free evolution without restraints (all analysis done with these frames)

These simulations were already performed by my co-supervisor and I had the trajectories that were to be analyzed at the beginning of my project.

2.2 Simulation of ArfB in solution

To understand the dynamics of the linker and the C-terminal tail in solution, I extracted the resolved ArfB structure from the cryo-EM complex. I preserved all the ions and water molecules within 20A of ArfB. This was then used as the starting structure to carry out dynamics as prescribed above to finally obtain a production run of 600ns (70-670ns). As outlined above, I carried out five independent runs of this system as well. These simulations were performed by me in the duration of my lab rotation.

2.3 Analyses

To extract certain features about the trajectories the GROMACS software tools were used extensively. This includes programs like *gmx rms* to compute root mean square deviation (RMSD) of structures along a trajectory from a starting structure, *gmx rmsf* to calculate root mean square fluctuations of residues averaged over the length of the trajectory obtained after fitting to the starting structure. These parameters give an idea of how dynamic and how stable the residues and the protein as a whole is during the simulation. *gmx do_dssp* was used to monitor secondary structure stability per residue in the course of the dynamics. This enables us to single out major structural changes. *gmx dist* was used to calculate pairwise distances between residues of interest and highlight possible interactions or motions, if persistent or not along the trajectory. *gmx covar* and *gmx anaeig* were used to perform principal component analysis (PCA) [15]. This is used to identify dominant modes of motion with respect to a set of atoms. The covariance matrix is calculated and diagonalized to obtain eigenvectors and eigenvalues. Trajectories can be projected along these eigenvectors to identify local motions along these coordinates, which are often difficult to observe due to smaller fluctuations in original trajectories. To plot the data obtained from the above analyses, I used python and xmgracee. These common analyses were performed for the three systems and will be discussed elaborately in the next sections.

3 Results and Discussion

3.1 ArfB in solution

Based on reported studies, I wanted to address questions regarding the structural dynamics of the C-terminal of ArfB in solution with respect to its secondary structure and how it could possibly scan a non-stop complex. I also wanted to compare the dynamics of the linker residues of ArfB in solution as opposed to in the complex to gauge any tension along the linker in the complex. Hence , I performed molecular dynamics simulation of free ArfB extracted from the cryo-EM structure as outlined in the methods. This was also done in order to gain insights about its behaviour in the absence of interactions with

the ribosome. This would also give an idea of its structure prior to ribosome entry which was unresolved in the experimental solution structure. Fig. 3 summarizes the root mean square deviation of each snapshot from the starting structure (0ns) for the production run of 600ns. High values of RMSD arise due to the highly mobile linker and C-terminal residues. The highly fluctuating RMSD could also mean that the simulations have not evolved completely to reach a stable conformation. Also, a snapshot of the final structure from all five independent simulations indicates a compacted structure due to folding of the linker region (residues 99-112) as compared to the initial.

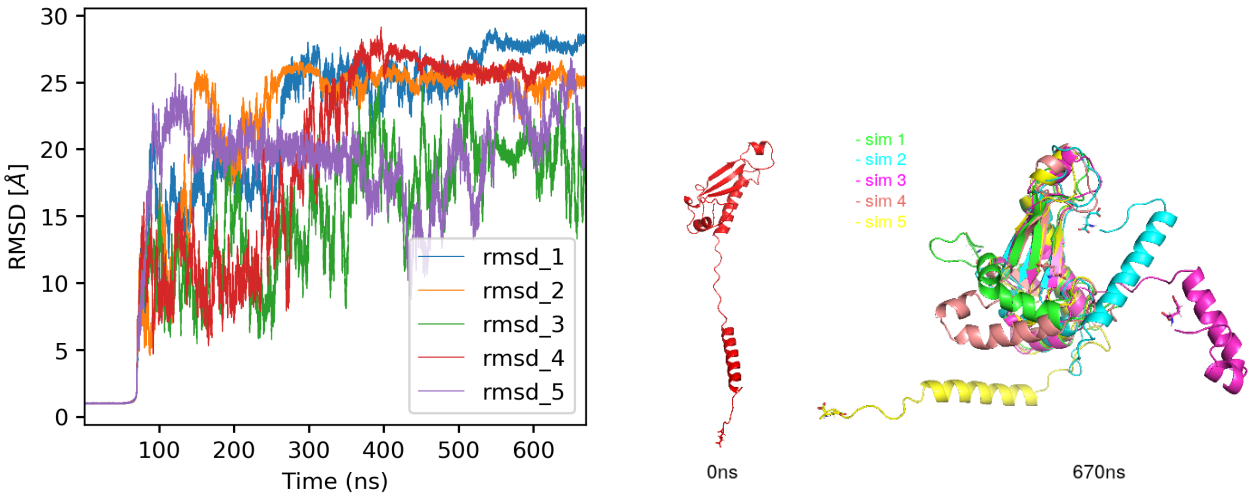


Figure 3: (i) Root mean square deviation of ArfB as a function of time with respect to 0ns structure (ii) Structural comparison of ArfB at 0ns (start) versus at 670ns (end) of the simulation

At the residue level, motions can be visualised in terms of root mean square fluctuations which are averaged for the duration of the trajectory. This gives an idea about regions that are more dynamic than others. As illustrated in Fig. 4, the RMSFs of 140 residues of ArfB were calculated by fitting the protein backbone atoms (C,O,N,CA) to the initial structure. The N-terminus includes residues 1-99, the flexible linker extends from residue 99-112 while the C-terminal tail includes residues 112-140. One caveat in this is that as the structure undergoes major structural rearrangements (the CTD in this case), RMSF measurements obtained by fitting to the entire intial structure would blow up for all the residues. This would mean particular domains like the NTD here, appear to be more dynamic that is really the case just because of poor fitting. This can be resolved by calculating the RMSFs for dynamically-similar behaving domains as indicated later on in Fig. 7. Based on the graph, we could say that the linker and C-terminal tail undergo major structural changes. The GGQ loop (residues 21-35) also appears to be more dynamic in the N-terminal domain. To further look into the secondary structure composition as a function of time, I used the program *gmx do_dssp*. This indicates local unfolding events in terms of loss of secondary structure in addition to the RMSF. In Fig. 5, we do see the instability of the C-terminal alpha-helix and of the GGQ loop as mentioned above. Upon further inspection, PCA reveals these features too. Principal component analysis helps to identify local domain motions which are difficult to visualize otherwise,

but contribute largely to domain rearrangements and hence the covariance matrix. The covariance matrix was calculated for the N-terminal domain and the C-terminal domain atoms respectively after fitting to the respective domain starting structure. The backbone atoms were used for fitting. I then obtained 100 conformations along the first eigenvectors obtained from diagonalizing above matrices. The trajectory along this new axis indicates the most dominant motion of the domain. Three frames from analysis of simulation 1 as shown in Fig. 3(ii) were picked from the 100 conformations to help visualise the dynamics.

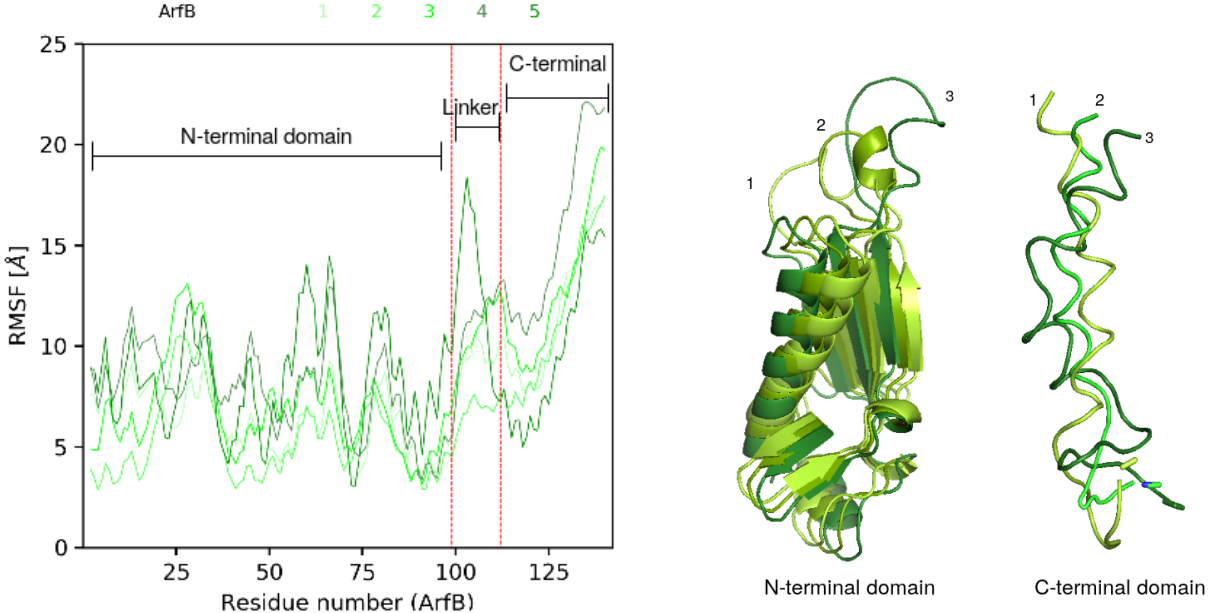


Figure 4: (i) RMSF of residues of ArfB averaged over the entire trajectory obtained by fitting to all the backbone atoms C,O,N,CA. Trajectories are numbered 1-5 and indicated in shades of green. (ii) 3 conformations sampled for the NTD and CTD separately from trajectories along 1st eigenvector of simulation 1. Respective eigenvectors were calculated from PCA after fitting to individual domains and calculating respective covariance matrices.

3.2 ArfB in ribosome complex

Based on the data available from the paper [9] I could now define a conformation of the GGQ motif in ArfB that attains the same distances as in the reactant state of PTH reaction. This would serve as a proxy condition for the ability to perform PTH hydrolysis. I defined two distances between Gln28 of ArfB ($^{26}GGQ^{28}$) and Phe77 of tRNA (2nd amino acid of the dipeptide):

$$Q28H(\text{ArfB})-\text{F77O}(\text{peptidyl-tRNA}) = 2.11\text{\AA}$$

$$Q28O\epsilon(\text{ArfB})-\text{F77H}(\text{peptidyl-tRNA}) = 1.98\text{\AA}$$

Based on these two distance measurements obtained from the trajectories using *gmx dist*, we were able to see a major difference between the "full" versus "cut" simulations. When distance measurement distribution from all the five simulations were plotted, We observed that many frames from the "full" trajectories were able to attain the defined QM-derived

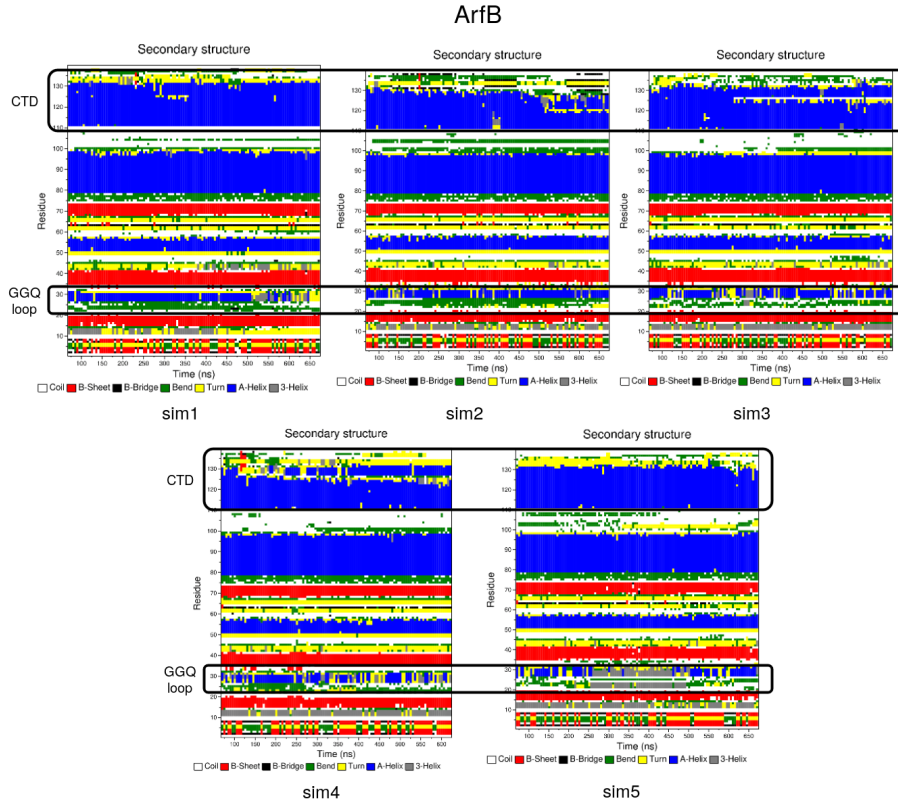


Figure 5: Secondary structure composition of ArfB as a function of time, with respect to individual residues indicated on the y-axis. Legends in blue indicate α helix, β sheet as red, coil as white, turn as yellow and bend in green. C-terminal domain residues 112-140 and of the GGQ loop residues 21-35 are highlighted in the boxes

distances, but no frame from the "cut" trajectory obtained the requisite distance. This result was obtained by my co-supervisor and my role has to look for plausible reasons for the same. Based on the hypothesis that the C-terminal tail exerts a pull/force to position the NTD in the right conformation (as I saw that when the linker is cut, the reactant state is not reached), this would be exerted via the joining linker. Hence, I looked at the pairwise distances of $C\alpha$ atoms of the linker residues from the "full" and "cut" trajectories. If the C-terminal domain indeed pulls on the N-terminal domain, we would expect a difference in the distribution as a pull would lead to consistently larger distances between residues. This is summarized in Fig 6. The adjacent $C\alpha$ atom distances overlap completely centering at about 3.8 Å. This is mostly because of the rigidity of the trans conformation across the peptide bond. In the case of alternate $C\alpha$ atom distances there is no particular trend across all pairs of measurements. This hints that a constant pull may not exist or other interactions with the ribosome might be playing some role and involve a more complex mechanism. I also looked at RMSF of residues after fitting to individual domains to see local fluctuations as reflected in Fig 7. Differences were observed in linker residues around the "cut" which would be natural due to increased degrees of freedom of motion and in the C-terminus end. No discernible pattern was seen based on the RMSF calculations alone.

Based on the above observations, I realised that gross analysis of parameters might

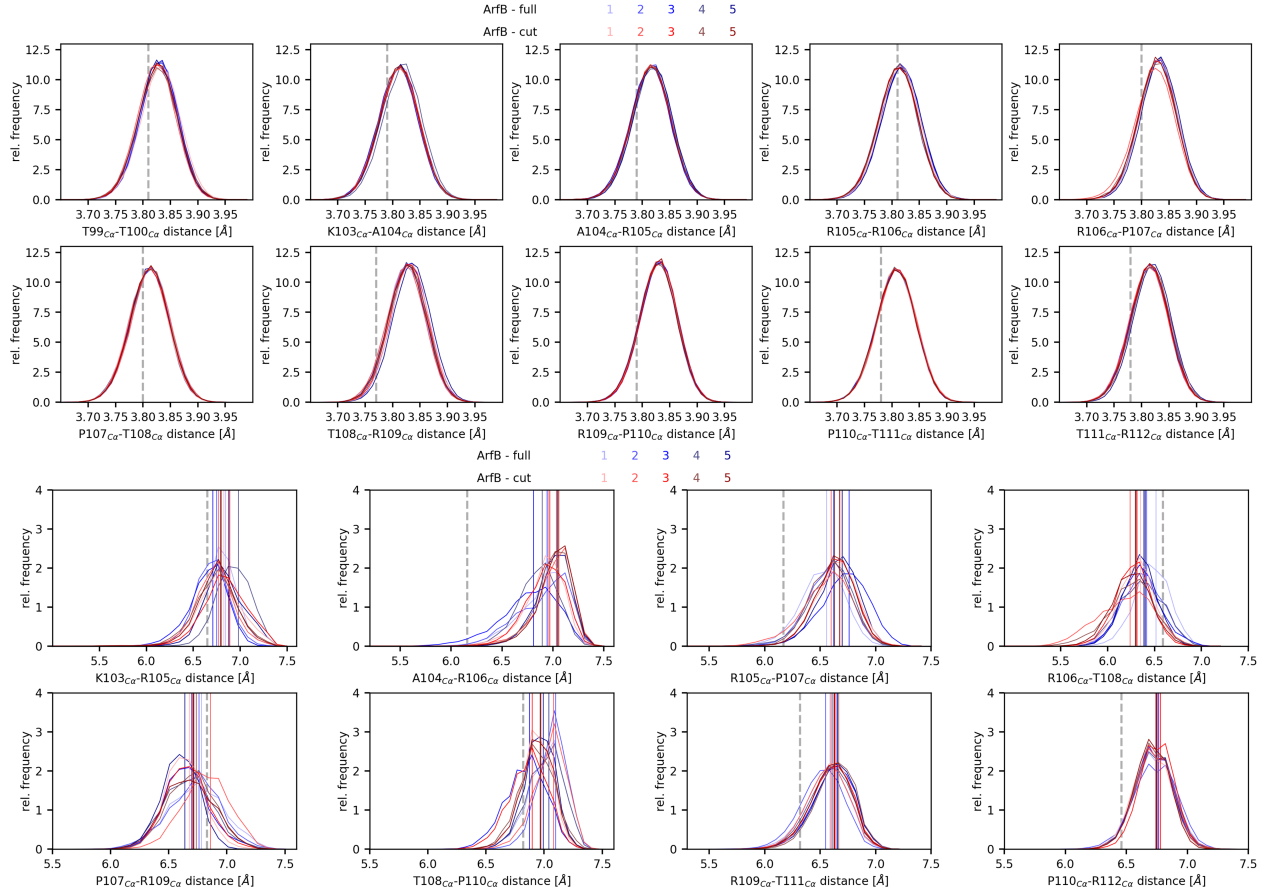


Figure 6: Histograms of C α distances between linker residues (99-112) obtained from "rib_arfb_full" and "rib_arfb_cut" simulations (i) top, 10 pairs of adjacent C α distances (ii) bottom, 8 pairs of alternate C α distances

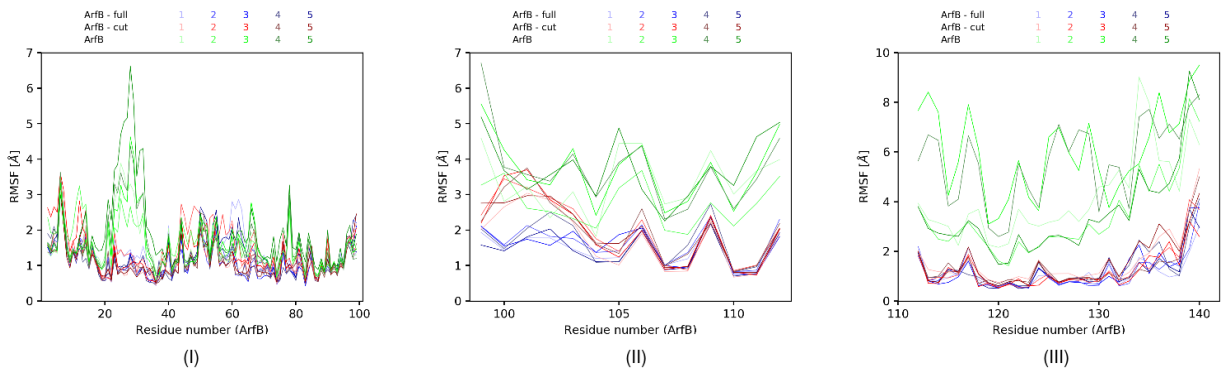


Figure 7: RMSFs of ArfB residues in "rib_arfb_full", "rib_arfb_cut" and "arfb" simulations (i) N-terminal residues(2-99) (ii) linker residues(99-112) (iii) C-terminal residues(112-140) obtained after fitting to their respective domains in the initial structure using backbone atoms

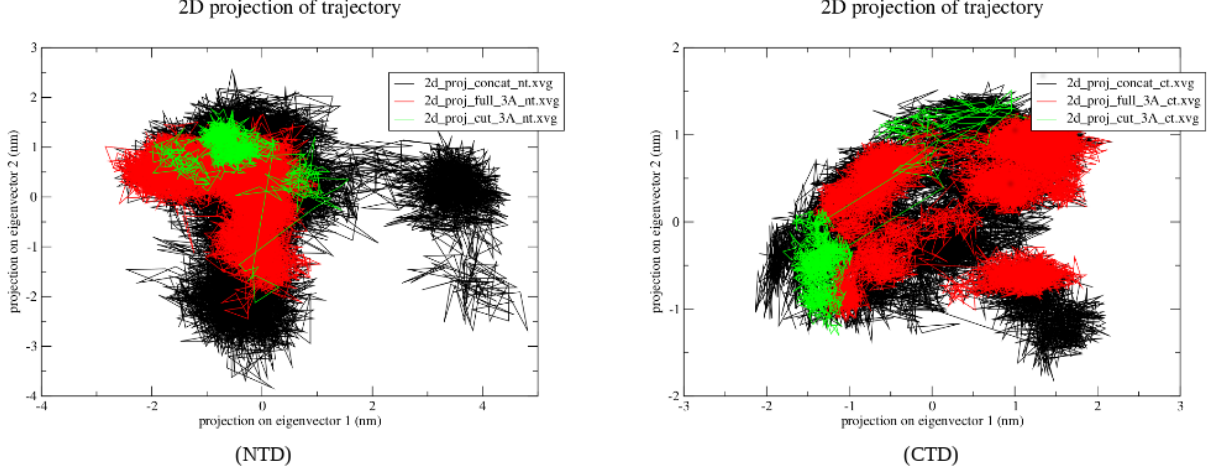


Figure 8: 2D projection of concatenated ("full"+"cut") trajectories along first two eigenvectors obtained from PCA of the same along (i) N-terminal domain (ii) C-terminal domain. Superimposed in red and green are subset frames of interest from "full" and "cut" simulations

overlook finer details. So I subset the ensembles of our interest from the larger trajectories based on the two QM distances (mentioned above) being less than 3Å. These new subset trajectories hence encompassed the few frames where the reaction state was reached in the case of "full" simulations and was tending to reach but did not in the case of "cut" simulations. The idea is to use PCA extensively to identify differences in local motions of small domains that clearly segregate "full" from "cut" frames of interest as described. To perform principal component analysis, I concatenated all the 10 simulations from "full" and "cut" into one. First, I used the N-terminal backbone to fit and calculate covariance of the same atoms and similarly for the C-terminal. I then projected all the individual trajectories, our frames of interest and the concatenated trajectory onto the 1st and 2nd eigenvectors obtained via diagonalization of the covariance matrices. Fig. 8 indicates preliminary results of the projection of the subset frames along the two corresponding eigenvectors. Black region indicates the projection of the concatenated trajectory, while red and green are regions traversed by the "full" and "cut" frames respectively. Based on projections from individual trajectories (not shown here), the motion along PC1 of the NTD motion was less significant as it described the motion that appeared in one specific trajectory alone ("cut_4" simulation). Motion along PC2 represents a bending motion involving the GGQ loop and will be of interest to further look into. With respect to the CTD motion there seems to be separation among the two sets of frames but the "cut" C-terminus wouldn't play a role per se as it lacks physical interaction with GGQ domain.

4 Conclusion

Based on the above studies, we were able to re-establish facts about the structural behaviour of ArfB in solution. This includes the unstructured C-terminal tail as seen from

the high values of RMSFs and the loss of secondary structure. This explains the unresolved CTD in the NMR structure of ArB in solution. The NTD on the contrary was stable in solution except for the GGQ loop that opens up in the absence of interactions with the ribosome. This suggests the important role of such interactions to preserve the secondary structure in order for catalysis to take place. The extended linker in the hydrophilic environment folds up as would be expected but the broader distribution of C α distances, indicated some pairs of residues being farther apart than in the complex. This hinted against the presence of tension along the length of the linker in the ribosome complex. From the QM distance comparisons, it is also quite evident that the C-terminal domain must be playing a role in physically positioning the GGQ domain for the catalysis to happen efficiently, although the coordinated role and sequence of events that lead to it need a more rigorous analysis. Based on the above results, we could say that a simple pulling mechanism is likely not in place. To identify dominant motions affecting the positioning of the GGQ motif, one could perform PCA of the GGQ loop or the loop and the dipeptide together. Projection of individual trajectories along the eigenvectors would most likely give a clear distinction between the "full" and "cut" trajectories. To visualize larger rearrangements that could occur due to sub-unit rotation, one could also perform PCA of domains of ArfB after fitting to the subunits of the ribosome (50S,30S). Also one could monitor specific interactions based on reported results like stacking and electrostatic interactions over the length of the trajectories. All these analyses would then broaden the understanding of internal motions that occur in the core of the ribosome and lead to PTH.

References

- [1] Kenneth C. Keiler and Heather A. Feaga. *Resolving nonstop translation complexes is a matter of life or death*. 2014. DOI: 10.1128/JB.01490-14.
- [2] Koreaki Ito et al. "Nascentome analysis uncovers futile protein synthesis in escherichia coli". In: *PLoS ONE* 6.12 (Dec. 2011). ISSN: 19326203. DOI: 10.1371/journal.pone.0028413.
- [3] Kenneth C. Keiler. *Mechanisms of ribosome rescue in bacteria*. May 2015. DOI: 10.1038/nrmicro3438.
- [4] Sean D. Moore and Robert T. Sauer. "The tmRNA System for Translational Surveillance and Ribosome Rescue". In: *Annual Review of Biochemistry* 76.1 (June 2007), pp. 101–124. ISSN: 0066-4154. DOI: 10.1146/annurev.biochem.75.103004.142733.
- [5] Yoshihiro Shimizu. "ArfA recruits RF2 into stalled ribosomes". In: *Journal of Molecular Biology* 423.4 (2012), pp. 624–631. ISSN: 10898638. DOI: 10.1016/j.jmb.2012.08.007.

- [6] Yoshihiro Handa, Noriyuki Inaho, and Nobukazu Nameki. “YaeJ is a novel ribosome-associated protein in *Escherichia coli* that can hydrolyze peptidyl-tRNA on stalled ribosomes”. In: *Nucleic Acids Research* 39.5 (Mar. 2011), pp. 1739–1748. ISSN: 03051048. DOI: 10.1093/nar/gkq1097.
- [7] Yuhei Chadani et al. “*Escherichia coli* YaeJ protein mediates a novel ribosome-rescue pathway distinct from SsrA- and ArfA-mediated pathways”. In: *Molecular Microbiology* 80.3 (May 2011), pp. 772–785. ISSN: 0950382X. DOI: 10.1111/j.1365-2958.2011.07607.x.
- [8] Maria T. Wesolowska et al. “Overcoming stalled translation in human mitochondria”. In: *Frontiers in Microbiology* 5.JULY (2014). ISSN: 1664302X. DOI: 10.3389/fmicb.2014.00374.
- [9] Masoud Kazemi, Fahmi Himo, and Johan Åqvist. “Peptide release on the ribosome involves substrate-Assisted base catalysis”. In: *ACS Catalysis* 6.12 (2016). ISSN: 21555435. DOI: 10.1021/acscatal.6b02842.
- [10] Matthieu G. Gagnon et al. “Structural basis for the rescue of stalled ribosomes: Structure of YaeJ bound to the ribosome”. In: *Science* 335.6074 (Mar. 2012), pp. 1370–1372. ISSN: 10959203. DOI: 10.1126/science.1217443.
- [11] Hiroyuki Kogure et al. “Identification of residues required for stalled-ribosome rescue in the codon-independent release factor YaeJ”. In: *Nucleic Acids Research* 42.5 (2014), pp. 3152–3163. ISSN: 13624962. DOI: 10.1093/nar/gkt1280.
- [12] Niels Fischer et al. “Structure of the *E. coli* ribosome-EF-Tu complex at <3 Å resolution by Cs-corrected cryo-EM”. In: *Nature* 520.7548 (Apr. 2015), pp. 567–570. ISSN: 14764687. DOI: 10.1038/nature14275.
- [13] Sander Pronk et al. “GROMACS 4.5: A high-throughput and highly parallel open source molecular simulation toolkit”. In: *Bioinformatics* 29.7 (Apr. 2013), pp. 845–854. ISSN: 13674803. DOI: 10.1093/bioinformatics/btt055.
- [14] Lars V. Bock, Michal H. Kolář, and Helmut Grubmüller. *Molecular simulations of the ribosome and associated translation factors*. Apr. 2018. DOI: 10.1016/j.sbi.2017.11.003. arXiv: 1711.06067.
- [15] Andrea Amadei, Antonius B M Linssen, and Herman J C Berendsen. *Essential Dynamics of Proteins*. Tech. rep. 1993, pp. 412–425.